ISTITUTO NAZIONALE DI FISICA NUCLEARE

Sezione di Perugia

INFN/AE-04/10
25 October 2004

THE EXTENSION AND SHAPE OF THE COLLECTING ZONES OF THE GALACTIC COSMIC RAYS FROM HELIUM TO IRON

Antonio Codino[1], François Plouin[2],

1) INFN and Dipartimento di Fisica dell'Universita degli Studi di Perugia, Italy
2) Former CNRS researcher, LLR, Ecole Polytechnique, Laboratoire Leprince-Ringuet, F-91128 Palaiseau, France

Abstract

Hundreds millions of cosmic-ray trajectories, from Helium to Iron, have been simulated in the galactic disk in order to calculate the mean distance of cosmic-ray sources from the Earth. The dominant parameters affecting this distance is the galactic magnetic field which makes cosmic-ray trajectories much longer, about 3 orders of magnitudes, than the physical distance from the source to the Earth.

The calculations indicate that cosmic-ray sources powering the local flux around the Earth are mainly disseminated along the regular magnetic field lines of the Galaxy. The spatial distribution of the sources form characteristic figures in the disk volume, the collecting regions of cosmic rays. Assuming cosmic-ray sources to be uniformly distributed in the disk of the Milky Way, at the arbitrary energy of 1 TeV/u, the typical length and width of these regions are 29.9 and 0.53 kpc for Helium and 20.0 and 0.27 kpc for Iron. The mean physical distance of cosmic-ray sources from the Earth turns out to be 3.5 kpc for Helium and 1.6 kpc for Iron.

*Published by **SIS–Pubblicazioni***
Laboratori Nazionali di Frascati

1 Introduction

Some observational facts would indicate that most cosmic rays reaching the Earth are generated in the Galaxy, most likely in the disk. Only at very high energy, above 10^7 GeV/u, a tiny fraction of the cosmic-ray flux is currently believed to come from the exterior of the Milky Way [1]. In this study, limited in the energy interval 0.2 to 5×10^4 GeV/u, the bulk of cosmic-ray sources is assumed to be located in the interior of the Galaxy. With this hypothesis two simple questions may be formulated regarding cosmic ion propagation, from region to region, in the Galaxy:

(I) What distance cosmic rays travel before reaching the solar cavity, the Earth ?

(II) How this distance does it depend on the nuclear species ?

The present calculation intends to answer these two questions by a full representation of the cosmic-ray trajectories in the Galaxy by computer simulation. The necessary algorithms to perform this study has been already employed in previous papers regarding proton and beryllium ions [2,3] and extragalactic antinuclei [4]. This particular study has been possible only by the use of a new computational procedure, described in Section 4, which reduces the computer time of the simulation.

Silently implied in the first question, is that cosmic-ray sources are well defined zones in space, inside the Milky Way. Traditionally, by the term source is meant the location, the site, in the Galaxy, where cosmic rays are accelerated. A number of galactic sites have been suggested as source candidates, primarily the circumstellar space around supernovae. In this calculation, as in many others, the extension of the sources is neglected and only pointlike sources are considered. The spatial distribution of the sources feeding cosmic rays to the local zone defines a galactic volume called in this paper collecting region or basin. The last term is vaguely reminiscent of the zone of a country drained by a river. The concept of collecting zone or basin has been recently introduced [5] in order to better investigate some measurable quantities of the galactic cosmic rays.

This calculation regards cosmic ions from Helium to Iron in the energy range 0.2 GeV/u up to 50 Tev/u. The determination of proton collecting zones is more involved than those of heavy ions, because, as demonstrated elsewhere (see figure 5 of reference [2]), cosmic protons generate numerous secondary protons which immensely complicate the analysis of the results. The high and low energy intervals are discriminated, $in\ primis$, by the role of ionization energy losses in dumping cosmic rays in the disk, and $in\ secundis$, by the relative high value of nuclear cross sections below 0.7 GeV/u. The basins at very high energy, beyond 10^{13} eV and up to 10^{19} eV , are determined in a forthcoming paper [6], which estimates the residence times of heavy ions in the Galaxy at these extreme energies. A short account of this study at very high energy has been recently anticipated

[7].

The set of assumptions adopted in this calculation are given in Section 2. Section 3 introduces the definition and concept of collecting zone, giving some specific examples illustrating forms and extensions of some cosmic-ray basins. Some general important results on the sizes of the basins are also given in this Section. The particular computational technique, which enables us to practically accomplish this study, is discussed in Section 4. Then, the basin extensions at high energy are reported in Section 5 and those at low energy in Section 6. Though the main focus of this paper regards the simulation of cosmic-ray trajectories in the Galaxy, as a new powerful computational technique, yet, in Section 7, the last one, some physical implications are highlighted.

To our knowledge, the results reported in this paper give, for the first time, both a systematic and detailed account of the collecting zones of cosmic rays which is hardly achievable by using the analytical models of the cosmic rays.

2 Basic assumptions of the calculation

Let us here briefly summarize the basic parameters governing the mean length of cosmic-ray trajectories in the Galaxy. The galactic magnetic field is the dominant parameter governing the length of cosmic-ray trajectories. Traditionally, the galactic magnetic field is thought of as a superposition of a regular and a chaotic component. It is characterized by its shape (spiral), intensity (3 μG) and the characteristic time variation, called chaotic component. In figure 1 is shown the line pattern of the spiral magnetic field referred also as regular field. The solid line which intercepts the local zone is called the principal field line. The field strength varies in the disk volume as previously reported [8] (see figure 2 of this reference). Cosmic ions propagate along the spiral magnetic field shown in figure 1, describing deformed helixes. They bounce forth and back along the regular magnetic field line with a modest diffusion in a direction perpendicular to the regular field. Thus, the propagation of a cosmic ray from the acceleration site to another arbitrary location of the Galaxy takes place by a diffusive motion and the algorithms for the propagation are described in detail elsewhere [2,8,9].

Besides the dominant role of the galactic magnetic field, both the gas density (1 hydrogen atom per cm^3 [10]) and the dimensions of the Milky Way have a prominent importance in the evaluation of the mean distance of the cosmic-ray sources from the solar cavity. The dimension of the disk, the position of the local galactic zone and the spiral field line intercepting the solar cavity are shown in figure 2. The Earth, the solar cavity or any instrument collecting cosmic rays is represented in the simulation algorithms by a sphere 100 pc in diameter, denoted local zone, placed at cylindrical coordinates r_S=8

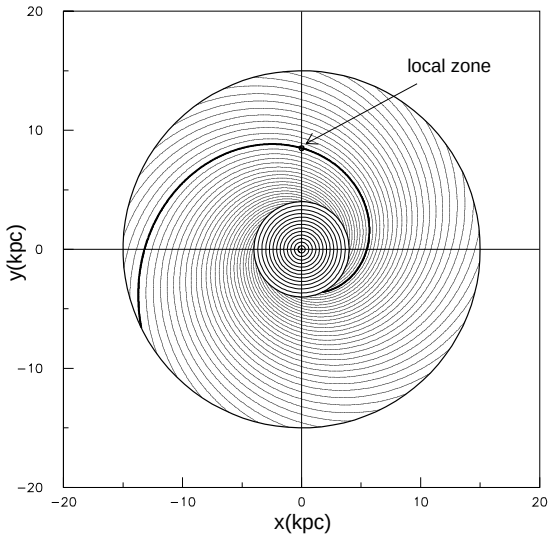

Figure 1: *Shape of the regular magnetic field in the Galaxy. The field lines are spirals extending from the bulge radius to the disk border. The solid line indicates a particular curve: that intercepting the local zone, concentric to the Earth. This curve is called principal magnetic field line.*

500 pc, z_S=0 and ϕ_S=90 $degrees$, as shown in the figures 1 and 2. This sphere is a computational device to perform appropriate averages of useful physical quantities.

A fourth fundamental parameter dominating the basic properties of cosmic rays in the disk, besides the magnetic field, the matter density and galaxy extension, is the inelastic nuclear cross section of a nuclide with the ambient matter of the interstellar medium, σ_N, characteristic of a given nuclear species. A physical quantity closely related to σ_N but more suitable than σ_N in this investigation, is the inelastic nuclear collision length, simply given by: λ_N = A/(N_A ρ σ_N). In figure 3 is shown, as an example, the quantity λ_N versus energy, for Carbon, between 0.2 GeV and 50 TeV/u.

The source distribution in the disk, referred as uniform, is sampled from the formula:

$$Q(r, z, l) = C\Theta(r - R)N(\sigma, z) \qquad (1)$$

where C is an appropriate normalization constant, $\Theta(r - R)$ is the radial distribution with a maximum radius R = 15 kpc and $N(\sigma, z)$ is the normal distribution in the z direction with a standard deviation σ of 80 pc. This spatial distribution has been used in a previous companion paper [2] along with the thin and supernovae distributions [11].

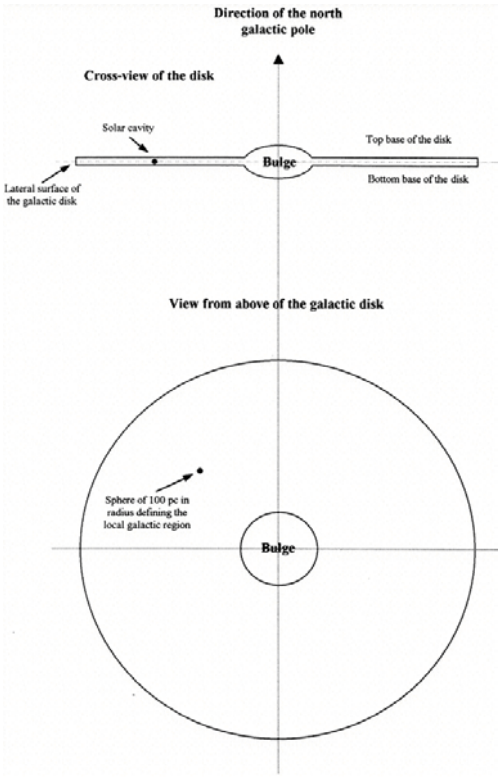

Figure 2: *Dimensions of the Galaxy incorporated in the simulation code. Side and top view of the Galaxy. The bulge is a symmetric ellipsoid, and the disk is a cylinder with a half-height 250 pc and a radius 15 kpc.*

3 Parameters defining the galactic basins of the cosmic rays

Let us define what is intended by collecting zone or basin. The coordinates of the source point of a cosmic ray are denoted r_s, ϕ_s and z_s where s stands for source or initial point of the trajectory. An instrument placed at the arbitrary location of the galactic disk with coordinates r_i, ϕ_i and z_i receives a cosmic-ray flux which has to originate at some points in the disk, belonging to the source distribution Q(r,z,ϕ) or another distribution. The collection of all points r_s, ϕ_s and z_s forms a spatial distribution called the source distribution related to the position of the detector, denoted by B(s,i), where B stands for basin. This distribution differs from the overall source distribution Q(r,z,ϕ) in the disk, because only a minority of the cosmic ions do actually reach the detector. Generally, a change in the position of the detector entails a change in B(s,i).

Though a full quantitative characterization of the basins is stored in the 3 dimensional function B(s,i), it is more useful, for a quick and crude evaluation of a basin extension, to take advantage of some global parameters related to B(s,i). The mean distance between the source and the instrument (or equivalently, detector, Earth, Sun, solar cavity and local zone) denoted by D_{si}, is determined and explicitly calculated using the concept

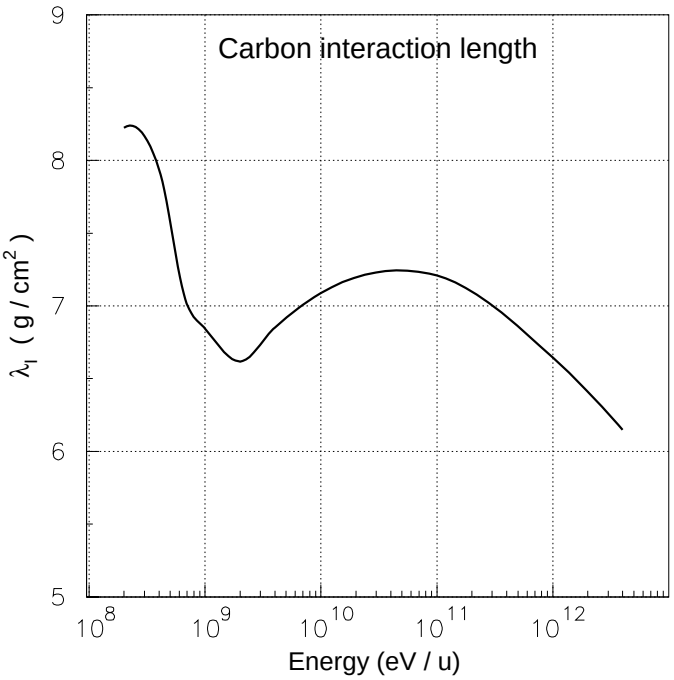

Figure 3: *Inelastic nuclear collision length of carbon versus energy from 0.2 up to* $50\,000$ GeV/u*. The inelastic cross sections of other ions such as* He*,* Al *and* Fe *have similar behavior.*

of collecting zone or basin. The projection of B(s,i) onto a suitable plane, for example the galactic midplane, may be visualized in a variety of ways.

In figure 4 are displayed, as an example, the bidimensional distribution of the iron sources feeding the local galactic zone. It turns out from figure 4, and similar calculations for other nuclides, that most cosmic rays arriving to the local galactic zone have sources disseminated along the principal field line of the spiral magnetic field. This important result has been previously obtained, in a variety of circumstances related to the physical and geometrical parameters of the Galaxy, for cosmic-ray protons and Beryllium. If the regular magnetic field, instead of being spiral, is ring or elliptical, the accumulation of the sources in a narrow strip along the principal field line persists as well [2,8].

An image of the source distribution of those iron nuclides intercepting the local zone is a useful tool, for an instant comprehension of the basin extension. Basins can be also represented by contour plots encompassing a predefined, arbitrary, appropriate amount of sources.

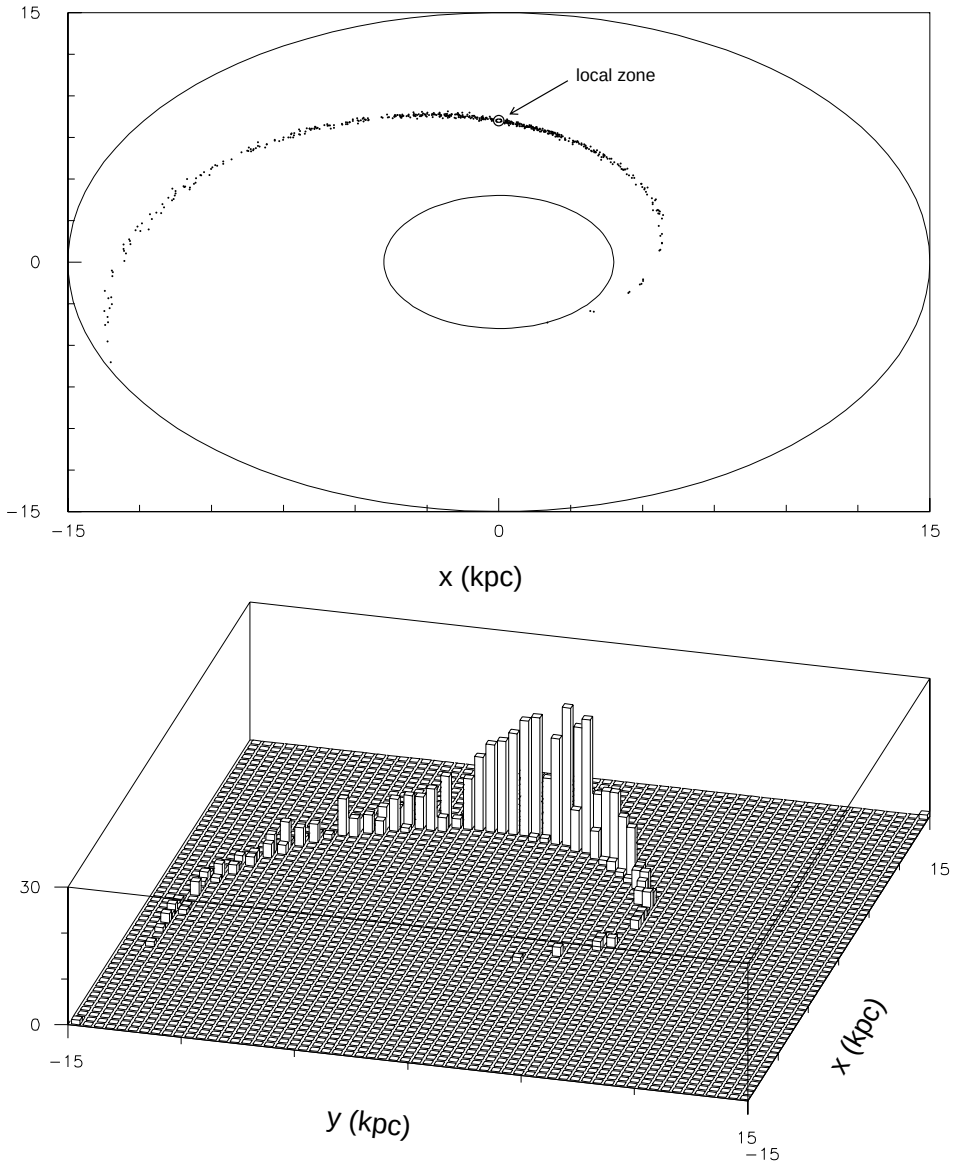

Figure 4: *Iron source distribution in the galactic disk with constant energy of 1 GeV/u powering the local galactic zone. Sources are predominantly located around the principal magnetic field line.*

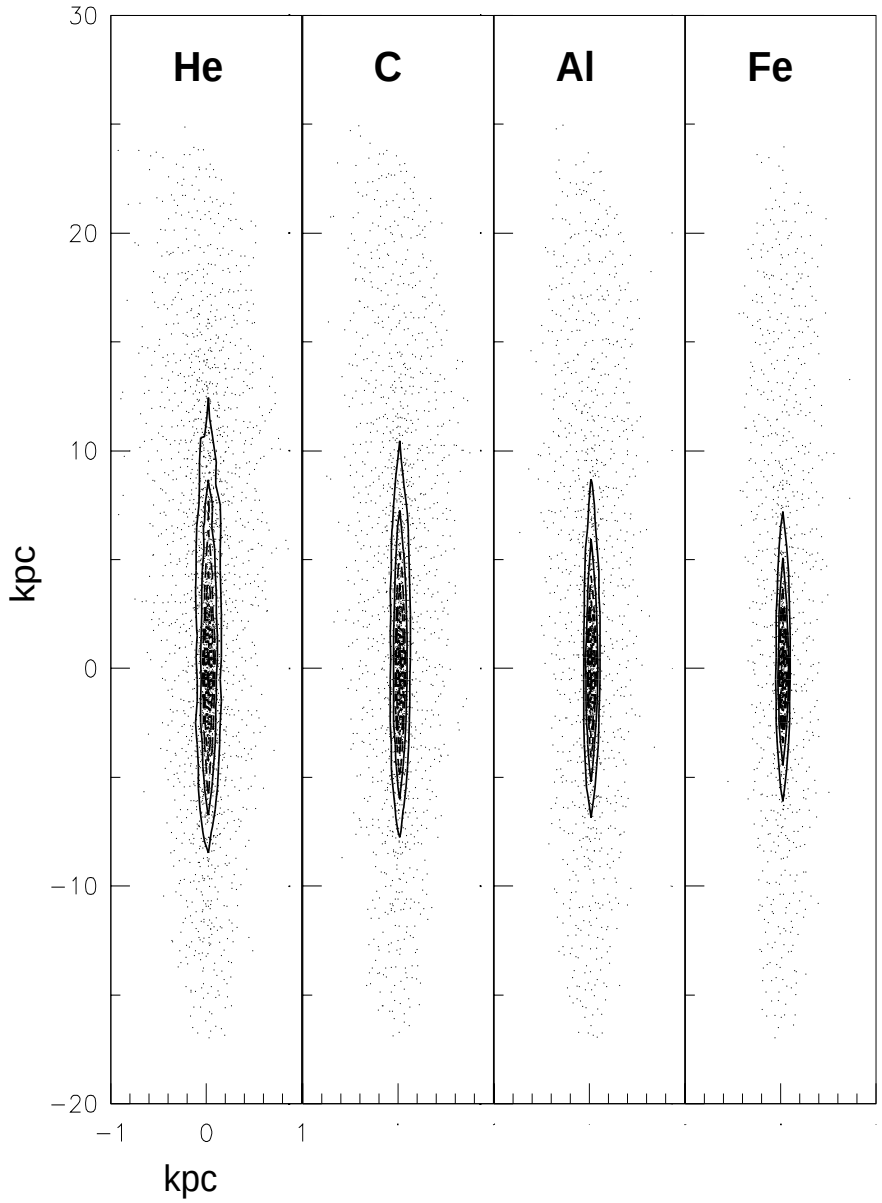

Figure 5-a

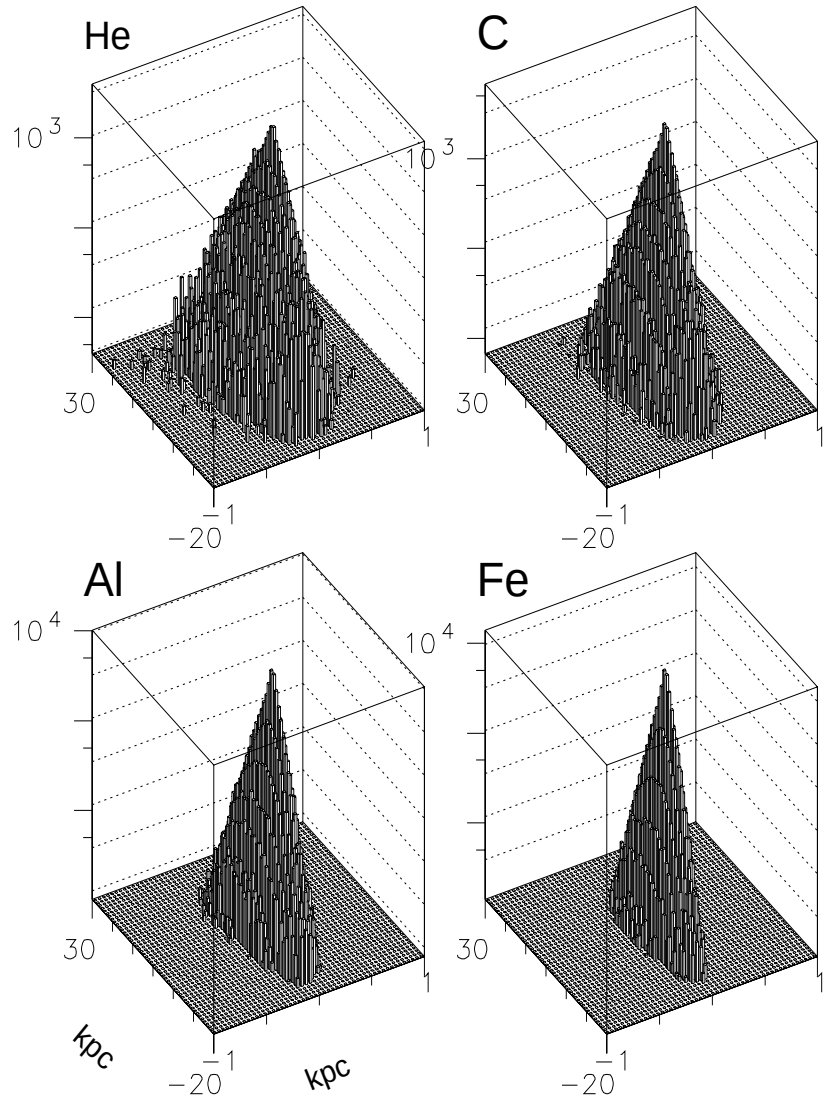

Figure 5-b

Figure 5: *Contour levels for He, C, Al and Fe illustrating the distribution of cosmic-ray sources feeding the local galactic zone. 5-a : The sources, which accumulate along the principal field line, are more concentrated for Iron than Helium. 5-b : The same data displayed in figure $5-a$ in a logarithmic scale which highlights the exponential nature of the distribution.*

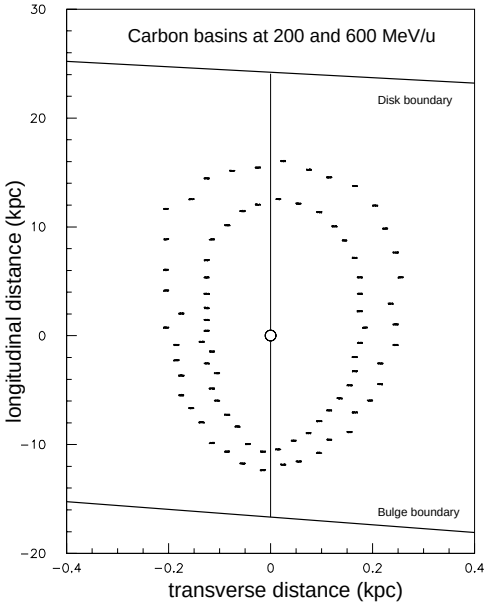

Figure 6: *Illustration of a basin of carbon ions for an observer located in the local galactic zone. The small circle at the center of the figure represents the Earth. The two dashed curves are the boundary of the carbon basins of kinetic energy of .2 and .6 GeV/u. In this energy interval the boundaries of the basins are mainly forged by the ionization energy losses.*

Event distribution, expressed by contour levels for Helium, Carbon, Aluminium and Iron, at 1 TeV/u, are displayed in figure 5-a. They are extracted from the general distributions B(s,i) projected onto the galactic midplane. These results give a simple and useful vista of a basin. In figure 5-b the same data are plotted in a logarithmic scale and the regularity of the distributions reflect the exponential nature (nuclear cross section and coherence length of the regular magnetic field) of the ion propagation at 1 TeV/u. The contour plots are drawn using the principal field line as reference axis. This choice facilitates a variety of cross-checks and a useful comparison with other magnetic field configurations.

In figure 6 the contour plots of the distribution B(s,i) for carbon ions of 200 and 600 MeV/u are displayed. In this case the contour plots include a fraction .90 of the sources and they are projections of B(s,i) onto the plane z=0, the galactic midplane. The principal magnetic field line is represented by a vertical solid thin line, while the local zone by an dot at the center of the figure 6. Note also that the scale of the horizontal axis differs from that of the vertical axis by a factor of 62.5.

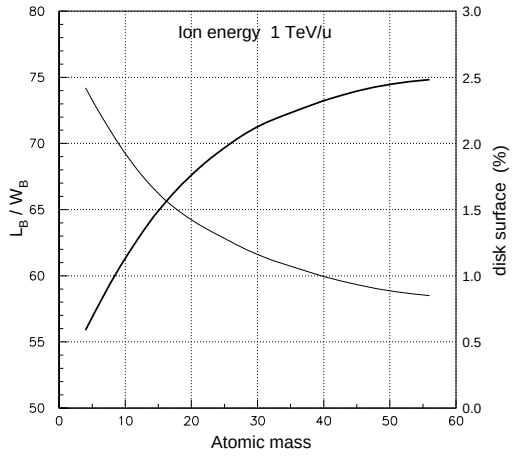

Figure 7: *Length-to-width ratio of galactic basins versus the atomic mass of the cosmic ions. The smoothness of the curves suggests that cosmic-ray basins have the same shapes.*

As far as the shapes of the basins are similar, or not very dissimilar, from those shown in figure 6, the dimensions of a basin may be characterized by its length, L_B, along the principal field line and its width, W_B, normal to the principal field line. For instance, L_B of the carbon basin at 600 MeV/u shown in figure 5, is 27.7 kpc and W_B is 0.46 kpc in a contour level of 90 per cent of the events. The dimension of the basin depends, patently, on the energy of the nuclides, besides other parameters. Note that the length of the principal field line (shown in figure 1) passing through the sun going from the bulge radius to the disk border is 40.73 kpc.

The ratios of the basin lengths to the widths, L_B/W_B, have been also calculated at the arbitrary energy of 1 Tev/u and the results reported in figure 7. The basin lengths L_B, extracted from contour plots analogous to those shown in figure 6, range from 20.0 kpc for Iron up to 29.9 kpc for Helium, as reported in figure 8. Thus, knowing the ratio L_B/W_B versus atomic mass, the basin widths may be roughly but safely evaluated without performing any detailed calculation , provided that L_B is known. Note also that L_B is approximately proportional to D_{si}, the mean distance of the sources from the solar cavity, which is simply defined by the arithmetic mean: $D_{si} = \sum_k^N d_{si}^k$ / N, where N is the total number of cosmic rays included in the mean and d_{si}^k, the mean distance of the generic source k from the instrument. In figure 8 is also shown D_{si} versus atomic mass of the cosmic ion. The quantity D_{si} is an overall, important characteristic of a basin but it ignores both the its form and profile; nevertheless its value offers another aspect of the general basin extension regardless of the form framed by L_B and W_B.

In short, the basin consists of a spatial region populated by a subset of galactic sources B(s,i) which is a part of the general source distribution Q(r,z,ϕ) given above. Notice that only the relative position between the instrument and the source distribution defines a basin once the magnetic field structure, interstellar matter density and geometrical boundaries of a galaxy are given.

4 Representation and inversion of cosmic-ray trajectories in a magnetic field.

The Earth or any instrument collecting cosmic rays are so small compared to the dimensions of the Galaxy that the calculation of any physical quantity pertaining cosmic rays intercepting the Earth is highly inefficient. For example, out of half million cosmic-ray trajectories propagated and reconstructed in the Galaxy only $4\ 000$ of them intercept the local galactic zone. In many cases, this small number of cosmic ions may not be sufficient to evaluate the desired physical quantities. This harsh aspect of trajectory simulation probably explains the persistence of the analytical models in the study of cosmic rays.

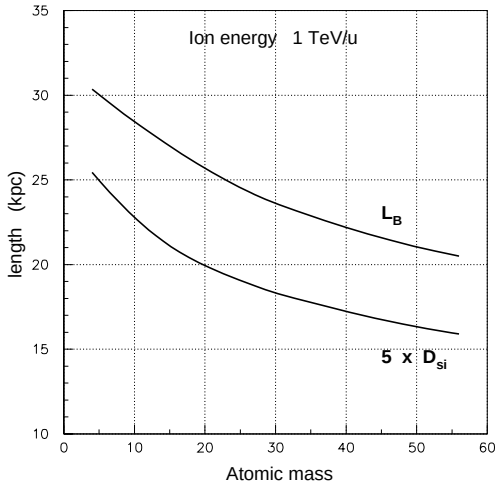

Figure 8: *Basin length versus atomic mass of cosmic ions at the energy of* $1\ TeV/u$*. Mean distance* D_{si} *between source and instrument versus atomic mass, at the same energy. Although the basin length* L_B *is longer than* D_{si} *approximately by a factor of 5, it retains the same shape of* D_{si} *versus atomic mass of the ion.*

In the previous companion paper [2] the large size of the local galactic zone, a sphere of 100 pc in diameter shown in figure 2, was primarily chosen to intercept the maximum number of trajectories thereby reducing the simulation time.

In order to enhance the number of events intercepting the local zone while preserving an adequate, small size, a new procedure of calculation has been devised and actually utilized in the present study. The dimensions of the basins evaluated in this paper takes advantage of the approximate reversibility of the trajectories in the propagation through the magnetic field of the Galaxy as explained below. Instead of using any plausible distribution of cosmic-ray sources and counting the particles reaching the local galactic zone, which is the natural, real mechanism of propagation, the reverse process is called into play. Particles are injected from the local galactic zone, a mere point in the Galaxy, and the end points of the trajectories memorized. The end points of the trajectories are regarded as the cosmic-ray sources. Thus, the initial points of the trajectories (sources) have been interchanged with the end points.

In order to quantitatively appreciate and cross-check the equivalence between the initial and final ends of a trajectory for the purposes of this study, the following procedures is proposed. Cosmic rays are injected along the principal field line, at varying distances from the local zone, as sketched in figure 9. They propagate in the disk volume through the magnetic field structure. A plane A perpendicular to the principal field line, placed at a given distance from the source as indicated in the same figure, is used to count those cosmic rays reaching it. Cosmic rays intercepting this plane are counted and the impact positions registered. In figure 9 the plane A is arbitrarily positioned in the local zone.

By this procedure the number of cosmic-ray trajectories to be simulated to accomplish this study is greatly reduced, and accordingly the computer time. Moreover, the local zone is reduced to a mere geometrical point, which is an advantage. The number of iron and helium ions intercepting the plane A as a function of the distance from the injection zone, referred to as a source, at the energy of 1 TeV/u for both nuclides, is reported in figure 10. They are called transmission curves since they provide us with the particle losses, or equivalently particle transmission, along the principal field line (the solid line in figure 9). The reverse process is then simulated. Helium and iron nuclides are injected from a set of sources positioned along the principal field line and those ions reaching the plane B counted. Let be N_B the number of cosmic rays reaching the plane B, and N_A those reaching the plane A. The quantity $(N_B - N_A)$ / N_B gives us a quantitative indication of how different are the transmission curves in the 2 senses of propagation. It turns out that N_B is approximately equal to N_A. The quantity $(N_B - N_A)$ / N_B is 0.01 at 3 kpc and does not exceed .03 at 9 kpc. This small figures are, by far, more precise than those required in the present study. The average trajectory lengths in the two situations are also equal within 3 per cent.

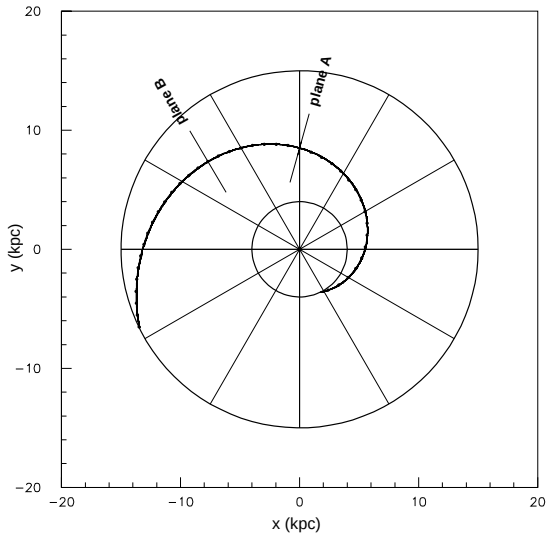

Figure 9: *Illustration of the calculation technique utilized in this study which interchanges the extreme ends of a cosmic-ray trajectory. Black dots along the principal field line represent cosmic-ray sources while the planes A and B are computational devices to count cosmic rays in two different circumstances as described in the text. There is an approximate equality in the fluxes of the cosmic rays reaching the two planes for an appropriate symmetric configuration of the sources.*

Generally, the number of particles reaching any plane τ normal to the principal field line, similar to planes A and B in figure 9, is controlled by the inelastic nuclear cross sections $\sigma_N(He)$ and $\sigma_N(Fe)$. At a given distance from any source, Helium is more abundant than Iron because $\sigma_N(Fe)$ is 750 mb at 1 TeV/u while $\sigma_N(He)$ is 102 mb at the same energy. If the inelastic cross sections of these 2 nuclides with the ambient matter are artificially equalized i.e. $\sigma_N(He)$=$\sigma_N(Fe)$, the resulting curves, analogous to those in figure 10, would become almost equal. However, the ratio of the cross sections cannot solely explain the particle transmission through the disk displayed in figure 10. In fact, a small fraction of cosmic rays overflows from the disk boundaries mainly along the z axis. Such fractions slightly differ between Helium and Iron. The transmission curves of the other nuclides with $2 < \mathrm{Z} < 26$, are comprised between those of Helium and Iron.

The reversibility of the trajectories is only approximate because the chaotic component of the galactic magnetic field operates a continuous and unpredictable perturbation of the particle trajectories. Of course, single trajectories connecting the source and instrument, and the reverse ones, connecting the instrument and source, are never equal but the mean values of some physical quantities may be

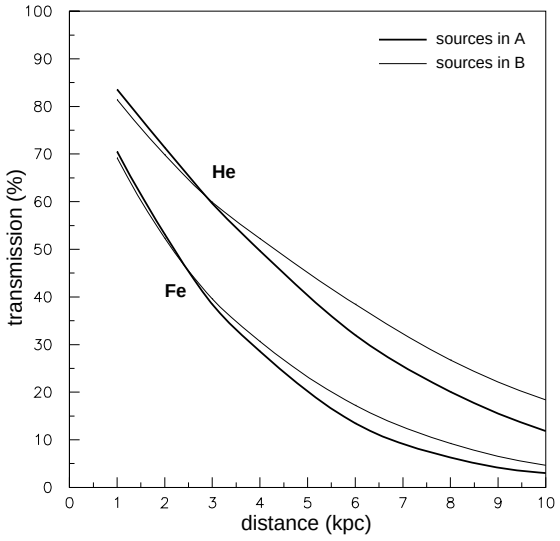

Figure 10: *Number of helium and iron nuclides crossing a plane perpendicular to the principal field line versus distance from the source, along the principal field line.*

equal. Typical physical quantities evaluated by this procedure are N_{AB} and N_{BA}, the impact point distributions of cosmic rays, the mean length between source and instrument D_{si}; namely, those quantities defining a cosmic-ray basin.

5 Basins at high energy

At high energy the effect of the ionization energy losses on the propagation of cosmic rays is negligible. As a consequence, only the inelastic nuclear collision lengths and the transverse propagation of cosmic rays determine the dimensions of collecting zones of cosmic rays. Otherwise stated, at high energy the determination of the basin extension is simpler than at low energy.

A quantitative characterization of the transverse propagation of cosmic rays with respect to the spiral field lines (see fig. 1) can be obtained by the same procedure adopted to determine the transmission curves of figure 10. In this particular calculation helium and iron sources are positioned along the principal field line as sketched in figure 9. This choice facilitates the analysis of the results.

The x and z distribution of the impact positions of iron and helium trajectories onto the plane τ is shown in figure 11. In this particular run sources are arbitrarily placed at 3.0 kpc from the local zone. A quantitative analysis of the two distributions indicates that the x-distribution is broader, being x the axis of the galactic midplane (see figure 2). An estimate of the widths of the distribution shown in figure 11 are

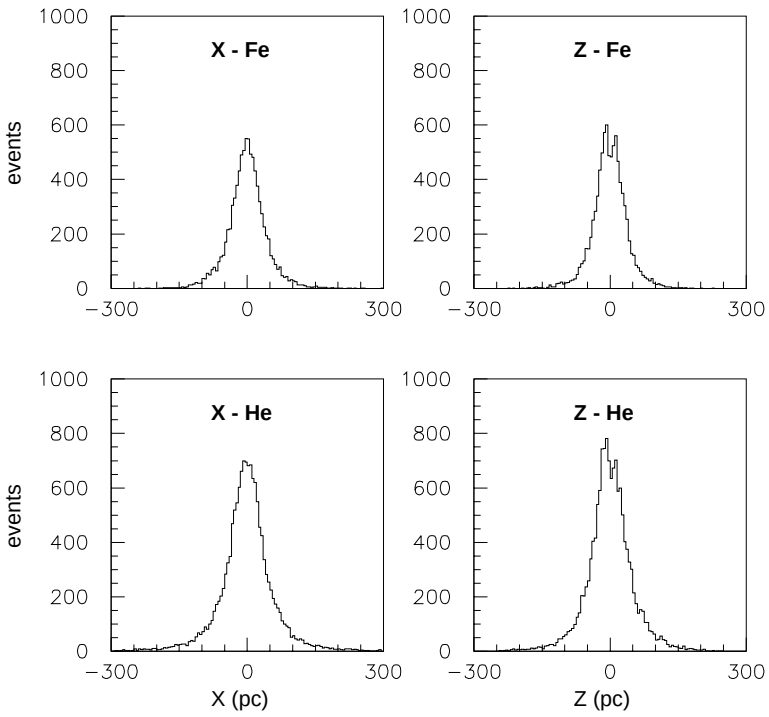

Figure 11: *Impact point distribution of cosmic ions crossing a plane normal to the principal field line. The x-distribution is a projection onto the galactic midplane while the z-distribution is a projection onto a plane normal to the galactic midplane.*

the standard deviations, σ_x and σ_z, of the projected distributions. In figure 12 the quantities σ_x and σ_z are plotted as a function of the distance from the source, arbitrarily placed along the principal field line, at the energy of 1 TeV/u. These quantities indicate the amount of the lateral spread of cosmic rays propagating along the regular magnetic field. For example, when the source distance from the Earth varies from 1 kpc to 5 kpc, the standard deviation changes from 25 up to 50 pc for Iron. The results in figure 12 are also indicative of how far cosmic rays propagate in a direction perpendicular to the principal field line.

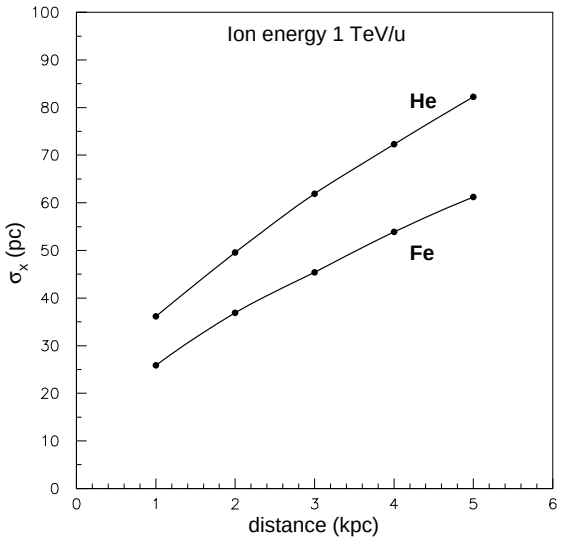

Figure 12-a

At high energy, once the gas density in the disk and the magnetic field configuration are assigned, the dimensions of the collecting regions are completely shaped by the inelastic nuclear collision length λ_N and disk thickness. This last quantity competes with the computed lateral spread σ_z, for cosmic ray containment. In order to appreciate the relative importance of these two parameters on the basin dimensions, let us envisage two extreme, ideal, possibilities. If the λ_N of any nuclear species would have been much longer than the disk extension, so that nuclear collisions would be rare in the disk volume, then the lengths and widths of the basins, L_B and W_B, would be controlled by the disk thickness, set at 250 pc for the Milky Way. In fact, in this case, most cosmic rays will migrate along the spiral field lines until their lateral spread σ_z exceeds the disk height. If the disk half thickness would have been much greater than 250 pc, so that cosmic rays, instead of traversing the disk boundaries, would undergo destructive nuclear collisions in the disk, the basin

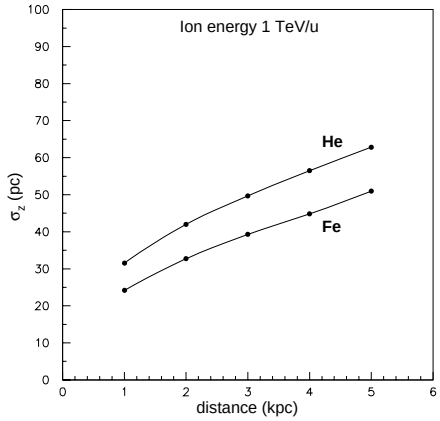

Figure 12-b

Figure 12: *Lateral spread of cosmic ions versus distance from the source along the principal field line in the x direction (12-a) and in the z direction (12-b).*

lengths would be totally controlled by the parameter λ_N. This is the second ideal possibility. In the Milky Way none of these two conditions are met for all the nuclear species, while for example, the Small Magellanic Cloud, due to its small diameter of 2.9 kpc, might conform to the first possibility.

In figure 13 the shapes and extensions of the basins at 1 TeV/u for Helium, Carbon, Aluminium and Iron are given. Samples of $2\times\ 10^5$ ion trajectories are simulated for each nuclear species. The contour plots, which are projections of B(s,i) onto the galactic midplane, include 90 percent of the particles emanated from the sources. The mean collision lengths of He, C, Al and Fe at the energy of 1 TeV/u are, respectively, 16.9, 7.8, 4.21 and 2.52 g/cm^2, while the basin lengths L_B in figure 13 are, respectively, 29.9, 27.8, 24.1 and 20.0 kpc. For comparison, the length of the spiral magnetic field line joining the solar cavity to the disk radius, as shown in figure 2, is 24.07 kpc, while that connecting the solar cavity to the bulge boundary is 16.66 kpc. Since λ_N varies with different cosmic ions, it is not a surprice that cosmic ions have different basin lengths. Thus the length of the helium basin at high energy referred to the Earth, is 73.4 per cent of the total length of the principal magnetic field line, which extends from the bulge radius to the disk border passing through the Earth, amounting to 40.73 kpc.

The hierarchy of the basin lengths against the atomic mass A of the four nuclides are reminescent of λ_N versus atomic mass but a simple relationship between λ_N and A is not evident.

Basins widths W_B are 0.53, 0.42, 0.28 and 0.27 kpc for He, C, Al and Fe, respectively. These widths are controlled by the intrinsic lateral spread of cosmic ion propagation shown in figure 12. The ratio L_B / W_B versus atomic mass, at the energy of 1 TeV/u, is given in figure 7. This ratio coupled with L_B versus atomic mass, given in the subsequent figure 8, would enable, if necessary, to determine the basin dimensions of other cosmic ions between Helium and Iron .

6 Basins at low energy

The total amount of matter traversed by cosmic rays before undergoing a complete stop, called range in experimental Nuclear Physics, is 53.6 g/cm^2 for Helium, 17.9 g/cm^2 for Carbon, 8.64 g/cm^2 for Aluminium and 4.48 g/cm^2 for Iron. These values refer to the initial kinetic energy of 0.5 GeV/u. Since the matter thickness of a typical basin in the Galaxy is in the range 5-20 g/cm^2 the importance of ionization energy losses at low energy is patent *a priori*. Also the particular shape of λ_N versus energy, reported in figure 3 for carbon ions, intervenes to govern the basin extensions at low energy. There is an abrupt decrease of λ_N between 0.2 and 0.7 GeV/u, a subsequent moderate decrease between 0.7 and 1.5 GeV/u followed by a rise up to about 50 GeV/u. These excursions of λ_N with energy have a remarkable effect on the basin extensions.

The trajectories of cosmic rays wandering in galactic volume have been subdivided into three classes depending on the manner cosmic ions disappear from the galactic disk. Nuclear collisions and ionization energy losses operate the destruction of cosmic rays in the disk volume. The corresponding trajectories terminated by these processes are referred as nuclear and ionization trajectories; they form the first two classes. Trajectories overflowing from the disk boundary form the escape trajectories, the third class. At low energy the influence of ionization energy losses on the trajectory length is dominant, and consequently, the extensions of the basins are greatly affected by the particular energy of the cosmic ions. The total average length of a trajectory sample in the disk , L_D, can be expressed by the sum of three parts as

$$L_D = f_N L_N + f_I L_I + f_E L_E$$

where the coefficients f_N, f_I and f_E are, respectively, the fractions of nuclear, ionization and escape trajectories and L_N, L_I and L_E the corresponding trajectory mean lengths. Of course, it must be:

$$f_N + f_I + f_E = 1$$

The fractions of cosmic-ray trajectories extinguished by ionization energy losses f_I is strongly decreasing with increasing energy as reported in figure 14 for Helium, Carbon, Aluminium and Iron. These trajectories are generated with a uniform distribution of sources in the disk volume and they are not related to an observer placed in the local zone. At energies below 200 MeV/u the fractions f_I tend toward unity implying that nuclear interactions and escape from disk boundary rarely occur.

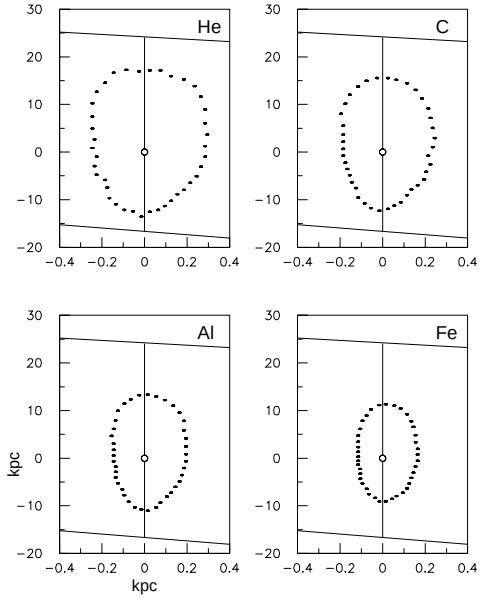

Figure 13: *Galactic basins for He, C, Al and Fe at the energy of 1 TeV/u. The vertical solid line is the principal field line, the top horizontal solid line is the disk boundary at* 15 *kpc and the bottom solid line is the bulge side at 4 kpc from the galactic center.*

In figure 15 is shown L_I versus energy for the four nuclides where L_I is the full physical length of trajectories extinguished in the disk by ionization energy losses.

In figure 16 are shown the basin extensions for carbon ions at four different energies. The basins lengths at the energies of 0.2, 0.4, 0.6 and 1.0 GeV/u are, respectively, 22.8, 26.1, 27.7 and 26.0 kpc to be compared with 27.8 kpc at 1 TeV/u. Below 0.5 GeV/u the dominant mechanism of extinguishing cosmic rays in the disk changes, from nuclear collisions to ionization energy losses. Nevertheless, in this energy interval the lateral spread of cosmic rays, quantified by the standard deviations σ_x and σ_y introduced in Section 4, results basically unchanged. Thus the basin widths reported in figure 16 do not greatly differ from those at high energy, at 1 TeV/u, shown in figure 13. The shapes of He, Al and Fe basins at low energy are similar to that of Carbon.

As suggested in Section 3, the physical distance D_{si} between the source and instrument, instead of L_B and W_B, may be also utilized to determine the basin extension. To this end, in figure 17, is plotted D_{si} versus energy for He, C, Al and Fe in the energy interval 0.2 - 2.5 GeV/u. The resulting curves exhibit a rapid increase, more pronounced for Helium than Iron, then the curves reach a broad maximum, and finally, they smoothly decrease toward a constant value. For example, D_{si} for Aluminium has a maximum of 3.9 kpc at 0.5 GeV/u, decreasing to

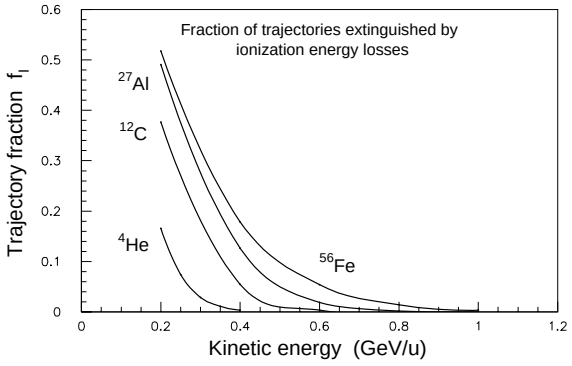

Figure 14: *Fractions of all trajectories extinguished in the galactic disk for Helium, Carbon, Aluminium and Iron as a function of the kinetic energy per atomic mass unit (MeV/u).*

the value of 3.5 kpc at 1.5 GeV/u and remaining constant up to 2.5 GeV/u. As far as the energy increases in the range 0.2 - 0.7 GeV/u more and more distant sources will feed any collecting instrument positioned in the local zone, and consequently, D_{si} increases with energy. Equivalently stated, the basin extension increases with energy as indicated in figure 5, in the case of carbon ions. After the maximum of D_{si} the slight decrease of the curves is due to the decrease of λ_N in the limited energy interval, 0.8-1.5 GeV/u as shown in figure 3 for Carbon. Notice that λ_N versus energy for He, Al and Fe behaves like that of C, namely, the minimum, maximum and changes of slope take place approximately at the same energies. However the decrease of D_{si} is modest, because particles coming from distant sources are a small fraction of the total number, as inferred from the transmission curves in figure 10.

7 Conclusions and remarks

The mean distances of cosmic-ray sources from the local galactic zone D_{si} for a variety of nuclides have been calculated and are reported in figure 8 at the energy of 1 TeV/u. In the energy interval 2 GeV/u up to 50 TeV/u, where the total inelastic cross sections versus energy are approximately constant (the maximum excursions are minor than 8 per cent), it turns out that helium sources are placed at a mean distance of 3.5 kpc while those of iron at 1.5 kpc for a uniform distribution of the sources. Comparable distances are expected for supernova remnant distributions [11,12] because the difference in the radial dependence with the distribution (1) is modest. The quantities D_{si} for other ions with $2 < \mathrm{Z} < 26$ lie between those of He and Fe shown in figure 8. The two dominant parameters controlling D_{si} are the total inelastic nuclear cross sections and the finite dimensions of the galactic disk,

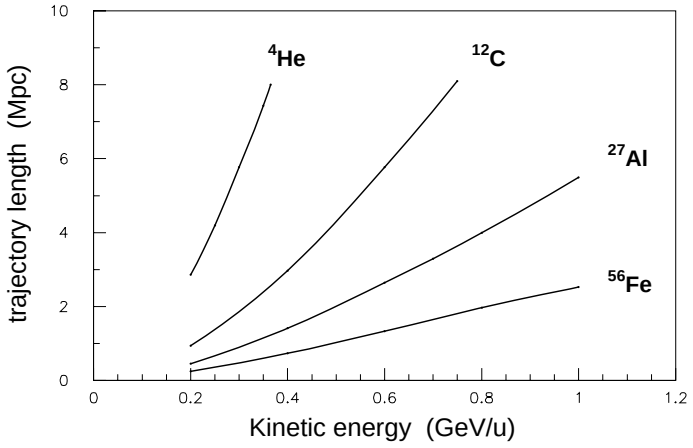

Figure 15: *Mean trajectory length of He, C, Al and Fe versus kinetic energy in the interval 0.2-1 GeV/u. The large differences in the four curves indicate the remarkable role of the ionization energy losses in dumping cosmic ions in the disk at very low energy.*

being 250 pc the half height, and 15 000 pc its radius.

At lower energies, below 1 GeV/u where ionization energy losses become the dominant mechanism to extinguish cosmic rays and where the inelastic cross sections have large and abrupt excursions with energy (see figure 3), the extensions of the collecting regions become smaller and smaller. This trend is illustrated in figure 4 for carbon ions where the basin lengths reduce from 16.5 to 13.6 kpc when the kinetic energy goes from 600 to 200 MeV/u, respectively. These results of the mean distance refer to the standard matter density in the disk of 1 atom *per* cm^3. The dimensions of the basins at very low energy indicate that, cosmic-ray sources feeding the local flux at Earth, are mainly located at distances of hundreds of parsec. Only along the principal magnetic field line, even at very low energy, there a is a dissemination of sources extending for several kiloparsec.

The dependence of D_{si} versus A confirms previous calculations regarding proton and beryllium trajectories in the Galactic disk [2, 3] which unambiguously indicated that proton sources are placed, on average, at greater distance from the solar cavity than beryllium sources.

The concept of the collecting regions not only facilitate the comprehension of some cosmic-rays properties but it has also simple, remarkable consequences. We cannot fail to mention some of them.

(I) The relative abundances of cosmic rays observed at Earth are heavily biased with respect to those existing in the Galaxy. This is easily inferred from the sizes of

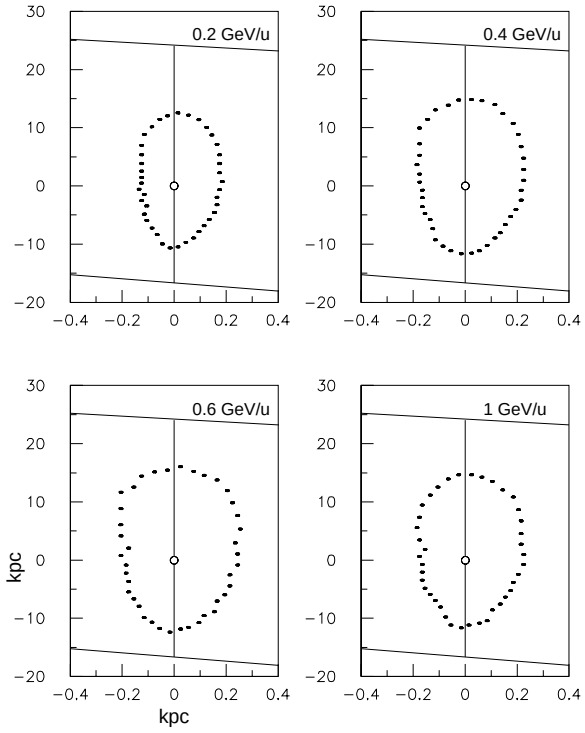

Figure 16: *Galactic basins of carbon ions at the energy of 0.2, 0.4, 0.6 and 1 GeV/u. The vertical line is the principal field line, the top horizontal line is the disk boundary at* 15 *kpc from the galactic center and the bottom line represents the bulge radius.*

the collecting zones, which are different for different ions. For example, for an equal number of iron and helium sources distributed according to equation (1), at the arbitrary energy of 10 GeV/u, the number of helium ions intercepting the local zone is a factor 2.7 higher than that of Iron. According to this result the helium-to-iron ratio measured at Earth, which is about 300 at 1 GeV/u, should be reduced by this factor of 2.7 at the sources. Thus, according to this calculation, there is much more cosmic-ray Iron stored in the Galaxy than local flux measurements at Earth would suggest.

(II) A notable aspect of the results reported in figure 8 is that different cosmic ions have very different collecting regions. The existence of the galactic magnetic field and the rates of nuclear collision for different ions causes trajectory lengths L_D to vary with A, the atomic mass of the ion. Because L_D is directly proportional to the grammage, it follows that different grammages are sensed by different nuclear species. This conclusion is opposite to that inferred by a variety of propagation models, called leaky box models, where all nuclear species with the same rigidity encounter the same grammage [13,14].

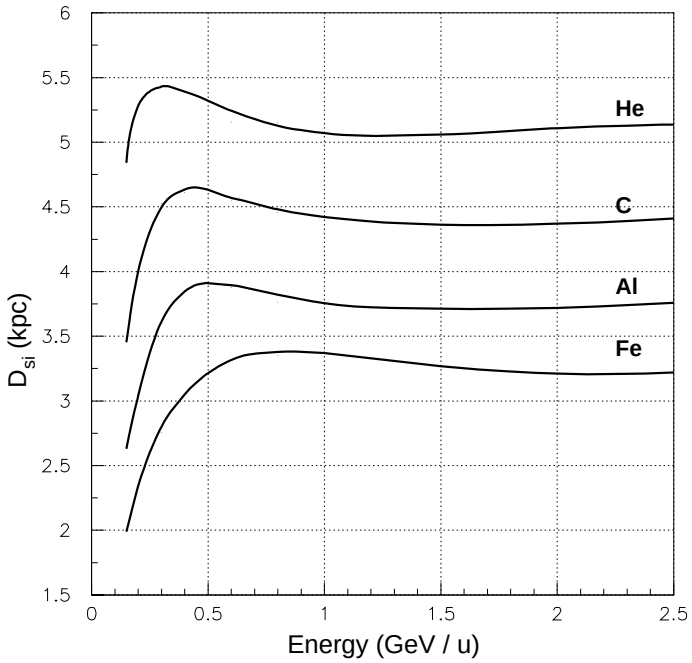

Figure 17: *Mean source distance versus energy from 0.2 to 2.5 GeV/u for Helium, Carbon, Aluminium and Iron. The distance D_{si} is evaluated in basins with contour plots including 90 per cent of the particles.*

(III) The basin extension can be determined once the source distribution in space and the position of the instrument are specified in a given magnetic field configuration. Suppose that extragalactic cosmic rays penetrate the disk arriving at Earth. What kind of basin will they form ? In figure 18 is summarized how this basin would look like according to the technique of calculation developed here. In order to reach the Earth any extragalactic cosmic ray must cross the disk boundaries. As a consequence, the lateral surface or the top or bottom surface of the disk, is crossed, at some point, by the extragalactic ion. In some respect the distribution of these points may be regarded as extragalactic sources even if the physical sources lie at larger distances, beyond the galactic halo boundary. Note also that, cosmic-ray sources of this example occupy a surface and not a volume, like all galactic sources involved in the previous figures. In figure 18-a is an overall view of such a basin projected onto the galactic midplane, which, not surprisingly, clusters along the principal magnetic field line. Figures 4, 18-a and 18-b vividly show that the main routes travelled by cosmic rays to depart from the Galaxy are the same routes to enter it. The x and z widths of this basin are much larger, about a factor of 8, than those reported in figure

4 regarding Iron at 1 GeV/u. In addition, the transmission curve along the principal field line, from the disk periphery to the Bulge, is rather flat, as shown in figure 18-b. A very interesting aspect of this basin is its grammage: the matter thickness sensed by the extragalactic cosmic rays while travelling through the disk volume. This grammage is totally different from that associated with galactic basins. In fact, on average, for Helium it amounts to 17.9 $g\ /cm^2$ while that sensed in the disk, distributed according to equation 1, is only 7.5 $g\ /cm^2$, at 1 Tev/u. A strong *caveat* is inferred from these and similar figures when investigating extragalactic cosmic rays, being antinuclei or extremely energetic cosmic ions. Almost all investigations on these topics ignore that the matter thickness traversed by extragalactic cosmic rays is much more conspicuous than that inferred using standard elaborations [15] of experimental data on boron-to-carbon flux ratio [16,17] or other similar secondary-to-primary flux ratios [18].

References

[1] Erlykin A. D. and Wolfendale A.W., Conference Proceeding, Vulcano Workshop, p. 467, 1998.

[2] Brunetti M.T. and Codino A., The Astrophysical Journal, 528, p. 789, 2000.

[3] Brunetti M. T. and Codino A., Proc. 25th Int. Cosmic Ray Conference , Vol. 4, p. 276, Durban, South Africa, 1997.

[4] Codino A. and Plouin F., Proc. 27th Int. Cosmic Ray Conference, Vol. 3, p. 239, Hamburg, Germany, 1997.

[5] Codino A. and Plouin F., Proc. 28th Int. Cosmic Ray Conference, Session OG.1, p. 1977, Tsukuba, Japan, 2003.

[6] Codino A. and Plouin F., The residence time of galactic and extragalactic cosmic rays around the knee, to be submitted to The Astrophysical Journal.

[7] Codino A. and Plouin F., Proc. 28th Int. Cosmic Ray Conf. Session HE1.2, p. 276, Tsukuba, Japan, 2003.

[8] Codino A., Conference proceeding, Vulcano Workshop, p. 439, 1998.

[9] Codino A., Brunetti M.T. and Menichelli M., Proc. 24th Int. Cosmic Ray Conference. Vol. 3, p. 100, Rome, Italy, 1995.

[10] Gaisser T. K., Cosmic Rays and Particle Physics, Cambridge, Cambridge University Press, 1990.

[11] Stecker S. W. and Jones F.C., Proceedings 12th ESLAB Symposium, 171, 1997.

[12] Esposito J.A., Pohl M. *et al*, The Astrophysical Journal, 507, p. 327, 1998 .

[13] Ormes J.F. and Protheroe R.J., The Astrophysical Journal, 272, p. 756, 1983.

[14] Cesarsky C.J., Proc. 20th Int. Cosmic Ray Conference , Vol. 8, p. 87, Moscow, Russia, 1987.

[15] Garcia-Munoz M. *et al*, The Astrophysical Journal, 64, p. 269, 1987.

[16] Orth C. D. *et al*, The astrophysical Journal, 226, 1147, 1978.

[17] Engelmann J.J *et al*, Proc. 17th Int. Cosmic Ray Conference , Vol. 9, p. 97, Paris, France, 1981.

[18] Engelmann J.J *et al*, Astronomy and Astrophysics 233, 96, 1990.

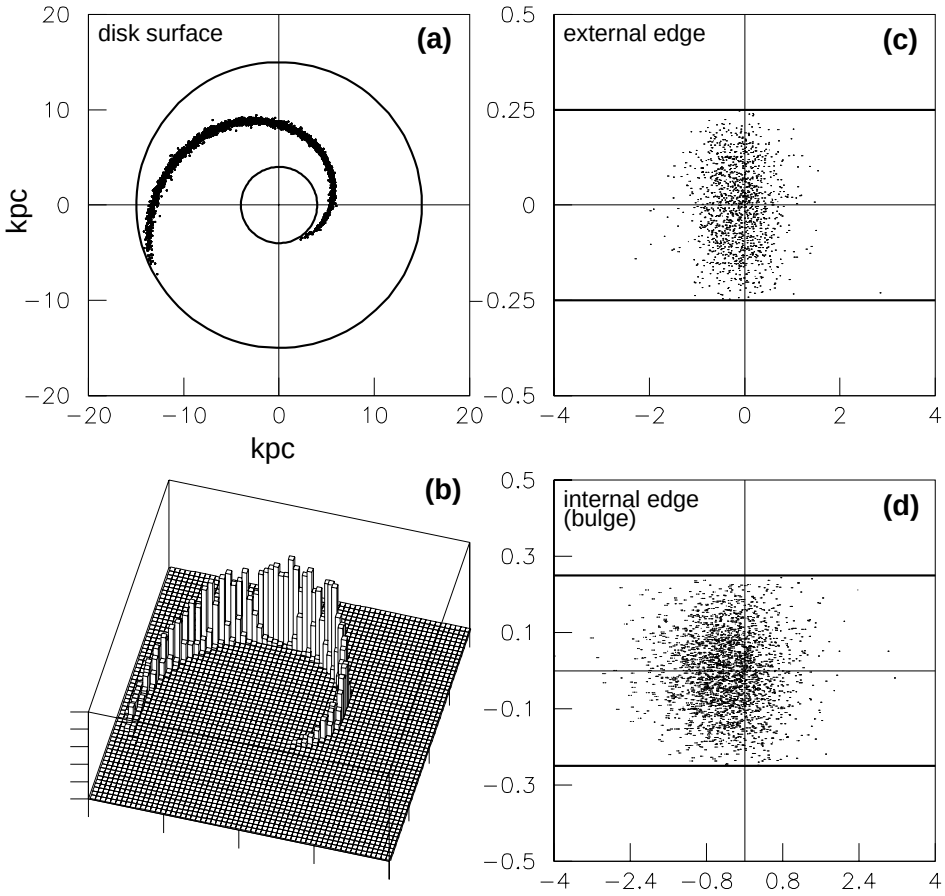

Figure 18: *Example of an extragalactic basin determined by injecting cosmic ions from the local galactic zone. As explained in Section 4, the reversibility of the initial and final points of the trajectories allows to determine the spatial concentrations of the sources ot the boundary of the Galaxy. 18-a Impact point distribution of cosmic ions flowing into the Halo by traversing the top and bottom surface of the disk. 18-b Profile of the same distribution reported in figure 18-a expressing the concentration of cosmic rays in a strip situated on the top and bottom surface of the disk. It is amazing that this strip follows, in a parallel manner, the principal magnetic field line. 18-c Impact point distribution of cosmic ions traversing the lateral surface of the disk and flowing into the Halo. 18-d Impact point distribution of cosmic ions entering the bulge side at 4 kpc from the galactic center.*